

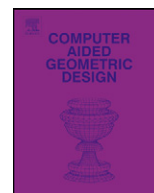


ELSEVIER

Contents lists available at ScienceDirect

## Computer Aided Geometric Design

www.elsevier.com/locate/cagd



## Curvature of singular Bézier curves and surfaces ☆

Thomas W. Sederberg<sup>a,\*</sup>, Hongwei Lin<sup>b</sup>, Xin Li<sup>c</sup><sup>a</sup> Department of Computer Science, Brigham Young University, Provo, UT 84602, USA<sup>b</sup> State Key Lab of CAD&CG, Zhejiang University, Hangzhou 310058, China<sup>c</sup> Department of Mathematics, University of Science and Technology of China, Hefei, China

## ARTICLE INFO

## Article history:

Received 20 February 2008

Received in revised form 21 February 2011

Accepted 21 March 2011

Available online xxxx

## Keywords:

Curvature

Singular points

Bézier curves

Bézier surface patches

## ABSTRACT

This paper presents a general approach for finding the limit curvature at a singular endpoint of a rational Bézier curve and the singular corner of a rational Bézier surface patch. Conditions for finite Gaussian and mean limit curvatures are expressed in terms of the rank of a matrix.

© 2011 Elsevier B.V. All rights reserved.

## 1. Introduction

The curvature at a point on a planar parametric curve  $(x(t), y(t))$  is given by

$$\kappa = \frac{|\dot{x}\ddot{y} - \dot{y}\ddot{x}|}{(\dot{x}^2 + \dot{y}^2)^{\frac{3}{2}}}. \quad (1)$$

At the point  $\mathbf{P}(0)$  on the Bézier curve in Fig. 1(a), we have  $\dot{x} = \dot{y} = 0$ , and therefore  $\kappa = \frac{0}{0}$ . We will refer to a point at which curvature is undefined as a singular point. If we plot the curve in Fig. 1(a) over the domain  $[-1, 1]$ , we see that  $\mathbf{P}_0$  is actually a cusp, as shown in Fig. 1(b). Fig. 1(c) plots curvature as a function of  $t$ , showing that the curvature goes to infinity as  $t$  approaches zero. This is true of most singular curves.

The curve in Fig. 2(a) is also singular and also has a cusp at  $\mathbf{P}_0$ . However, the curvature plot in Fig. 2(c) reveals that the curvature in the neighborhood of  $\mathbf{P}_0$  is finite, and the curvature at  $t = 0$  is a removable discontinuity.

Fig. 3(b) shows a special case of a singularity in which the entire curve is doubly traced because  $\mathbf{P}(t) = \mathbf{Q}(t^2)$ . The conditions for this are  $\mathbf{P}_0 = \mathbf{P}_1 = \mathbf{Q}_0$ ,  $\mathbf{P}_2 = \frac{2\mathbf{Q}_0 + \mathbf{Q}_1}{3}$ ,  $\mathbf{P}_3 = \mathbf{Q}_1$ , and  $\mathbf{P}_4 = \mathbf{Q}_2$ . As illustrated in Fig. 3(c), the curvature at the singularity  $t = 0$  is again a removable discontinuity, and the curvature plot is symmetric.

We define a singular corner point of a Bézier surface patch  $\mathbf{P}(s, t)$  to be an  $(s, t)$  pair at which Gaussian, mean, or normal curvature is undefined because one or more directional derivatives vanish. These points can occur in numerous ways, such as when  $\mathbf{P}_{00} = \mathbf{P}_{10}$  (so  $\mathbf{P}_s(0, 0) = 0$ ), or when  $\mathbf{P}_{01}$ ,  $\mathbf{P}_{00}$  and  $\mathbf{P}_{10}$  are collinear but not coincident ( $\mathbf{P}_s$  and  $\mathbf{P}_t$  do not vanish but their cross product does). The limit curvature for a singular point on a surface is usually infinite and can create complicated geometry, as illustrated in Fig. 4. However, conditions exist under which Gaussian and mean curvatures have a unique, finite

☆ This paper has been recommended for acceptance by G.E. Farin.

\* Corresponding author.

E-mail addresses: tom@cs.byu.edu (T.W. Sederberg), hwlin@cad.zju.edu.cn (H. Lin), qingwxin@gmail.com (X. Li).

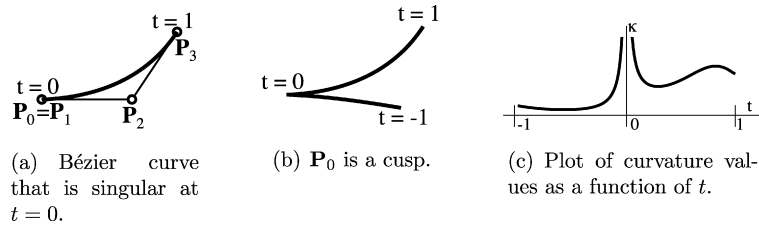


Fig. 1. Generic singular Bézier curve with infinite curvature.

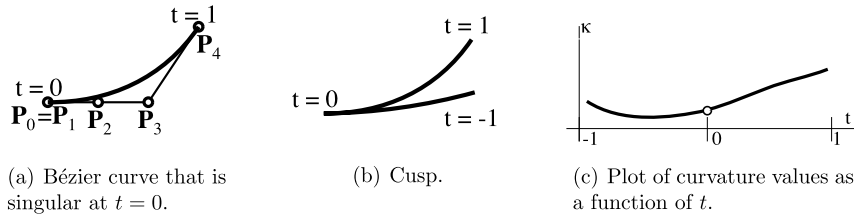


Fig. 2. Bézier curve with removable discontinuity in the curvature function.

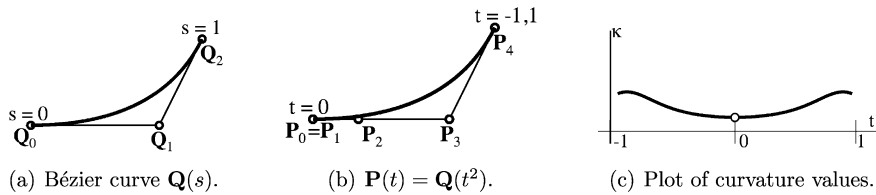


Fig. 3. Improperly parametrized Bézier curve  $P(t) = Q(t^2)$ .  $P(t)$  is doubly traced.

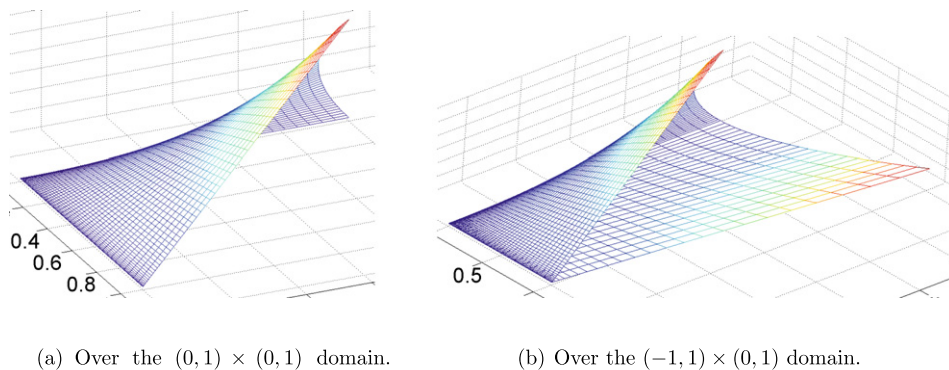


Fig. 4. Surface  $x = s^2 - st^2$ ,  $y = t^2$ ,  $z = s^2t^2$  is singular at  $(s, t) = (0, 0)$ .

limit (i.e., a removable discontinuity) at a singular point. This paper presents necessary and sufficient conditions under which this happens.

Singular corners have several practical applications in CAGD, such as representing an octant of a sphere using a tensor-product patch for which an edge collapses to a point. Singular corners also occur at extraordinary points in TURBS surfaces (Reif, 1998).

Analyzing the curvature of a generic singular surface is not straightforward. For example, the following approaches are not tenable:

- Apply the traditional equations for curvature based on differential geometry (Do Carmo, 1976) and then resolve the resulting  $\frac{0}{0}$  using L'Hospital's rule. Unfortunately, no version of L'Hospital's rule exists for functions of two variables.
- Perform a reparametrization (Reif, 1998). If a singular curve has the special form  $P(t) = P_0 + P_k t^k + P_{2k} t^{2k} + O(t^{2k+1})$  with  $k > 1$ , we can substitute  $t = u^{\frac{1}{k}}$  to obtain a non-singular curve  $P(u) = P_0 + P_1 u + P_2 u^2 + \dots$  and curvature can be computed conventionally. Note the requirement  $P_{k+1} = \dots = P_{2k-1} = 0$ . This approach can also be used for some singular surfaces, but only ones that honor similar restrictions.

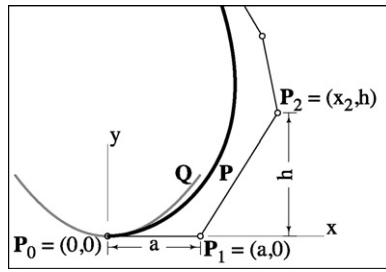


Fig. 5. Rational Bézier curve.

- Perform a local expansion of the form  $z = f(x, y)$ , then analyze the curvature of the expansion. But such an expansion does not exist in general, such as the example  $x = s^2 - st^2, y = t^2, z = s^2t^2$  in Fig. 4.
- Implicitize the singular surface and compute the curvature as in Goldman (2005). Since the implicit equation for a degree  $m \times m$  tensor-product surface is of degree  $2m^2$ , this approach is intractable. Furthermore, the implicit equation of a singular parametric surface often has vanishing partial derivatives that cause the formulae in Goldman (2005) to be undefined.
- Examine the limit curvature as the singularity is approached from any direction. This works in theory, but the resulting algebraic expressions are unwieldy.

Curvature at singular points has been studied in a few special cases, but no general treatment exists. Wolter and Tuohy (1991) analyze curvature for the case in which all control points on one boundary of a tensor-product Bézier surface patch collapse to a point, although the solution does not allow second-order anomalous curves (defined in Section 4). Singular patches are also mentioned in Bohl and Reif (1997), Hogervorst and van Damme (1993), Neamtu and Pfluger (1994), Pfluger and Neamtu (1993), Reif (1995). Curvature at the singular corner of a “ $D^2$  patch” is derived in Reif (1998), but the paper gives no general solution to curvature at a surface singularity, remarking that the general solution involves “extremely complicated non-linear necessary conditions”.

We present a general solution in terms of linear equations that are not extremely complicated. Our method is based on the concept of *order-of-contact* (Snyder and Hutchinson, 1902; Bruce and Giblin, 1984). Section 2 reviews the concept of order-of-contact and describes how the method can be adapted for singular points. Formulae are derived in Section 3 for curvature at a singular endpoint of a rational Bézier curve. Section 4 discusses tangency of singular surfaces and Section 6 discusses curvature of general singular surfaces.

## 2. Order-of-contact

Given a non-singular parametric curve  $\mathbf{P}$  defined in homogeneous form  $(x(t), y(t), w(t))$ , where the Cartesian coordinates of points on the curve are  $(x(t)/w(t), y(t)/w(t))$ , and a second non-singular curve  $\mathbf{Q}$  given in implicit form as a homogeneous polynomial equation  $q(x, y, w) = 0$ , the roots of  $f(t) = \mathbf{P} \circ \mathbf{Q} = q(x(t), y(t), w(t)) = 0$  are the parameter values of the points at which  $\mathbf{P}$  intersects  $\mathbf{Q}$ . If  $f(t) = f'(\tau) = \dots = f^{(k-1)}(\tau) = 0$  and  $f^{(k)} \neq 0$ ,  $\mathbf{P}$  and  $\mathbf{Q}$  are said to have order-of-contact of  $k$  at  $t = \tau$  (Bruce and Giblin, 1984). If  $x(t), y(t)$ , and  $w(t)$  are polynomials (as they are in this paper), then order-of-contact is equivalent to root multiplicity of  $f(t)$ . If  $\mathbf{P}$  and  $\mathbf{Q}$  have at least second-order contact at a point, they are tangent to each other and if they have at least third-order contact at a point, they have the same curvature at that point (Bruce and Giblin, 1984). This provides a tool for analyzing curvature, as we now illustrate using a rational Bézier curve with control points  $\mathbf{P}_i = (x_i, y_i)$ , weights  $\omega_i$ , and equation in homogeneous form

$$\mathbf{P}(t) = (x(t), y(t), \omega(t)) = \sum_{i=0}^n \omega_i (x_i, y_i, 1) B_i^n(t). \tag{2}$$

Choose a Cartesian coordinate system such that  $\mathbf{P}_0 = (0, 0)$ ,  $\mathbf{P}_1 = (a, 0)$ , and  $\mathbf{P}_2 = (x_2, h)$ , as shown in Fig. 5.

Let  $\mathbf{Q}$  be a parabola with homogeneous equation

$$q(x, y, w) = c_1x^2 - c_2yw = 0. \tag{3}$$

Then,

$$f(t) = q(x(t), y(t), w(t)) = \sum_{i=0}^{2n} f_i B_i^{2n}(t) \tag{4}$$

where

$$f_i = \sum_{j_1+j_2=i} \frac{\binom{n}{j_1}\binom{n}{j_2}}{\binom{2n}{i}} w_{j_1} w_{j_2} (c_1 x_{j_1} x_{j_2} - c_2 y_{j_2}). \tag{5}$$

Since  $f_0 = f_1 = 0$ ,  $\mathbf{P}$  and  $\mathbf{Q}$  have at least second-order contact and thus are tangent at  $(0, 0)$ . If non-singular  $\mathbf{P}$  and  $\mathbf{Q}$  meet with third-order contact, they are said to osculate, and  $\mathbf{Q}$  is an osculating parabola. Third-order contact requires

$$f_2 = \frac{c_1 a^2 n^2 \omega_1^2 - c_2 \frac{n(n-1)}{2} \omega_0 \omega_2 h}{\binom{2n}{2}} = 0.$$

This is satisfied if

$$\frac{2c_1}{c_2} = \frac{n-1}{n} \frac{\omega_0 \omega_2}{\omega_1^2} \frac{h}{a^2}. \tag{6}$$

By coincidence, the curvature of  $\mathbf{Q}$  at  $(0, 0)$  is  $\kappa = 2c_1/c_2$ . Since (6) assures third-order contact, the curvature of  $\mathbf{P}$  at  $\mathbf{P}_0$  is

$$\kappa = \frac{n-1}{n} \frac{\omega_0 \omega_2}{\omega_1^2} \frac{h}{a^2}. \tag{7}$$

This is the well-known equation for curvature at the non-singular endpoint of a rational Bézier curve (Farin, 1997, p. 176), which provides beautiful geometric insight.

It is worth noting that the derivation of (7) using order-of-contact requires much less work than a derivation based directly on Eq. (1).

### 3. Singular rational Bézier curves

We now adapt the method of order-of-contact in analyzing tangent and curvature at the endpoint of a singular rational Bézier curve (2) where

$$\mathbf{P}_0 = \dots = \mathbf{P}_{k-1} = (0, 0) \neq \mathbf{P}_k, \quad \text{with } k > 1, \omega_0, \omega_k > 0. \tag{8}$$

Section 3.2 describes a preprocess for dealing with zero weights.

**Theorem 1.** For a singular rational Bézier curve (8), the tangent line at  $\mathbf{P}(0)$  is  $\mathbf{P}_0\mathbf{P}_k$ .

**Proof.** Consider the family of lines passing through the origin:

$$q(x, y, w) = ax + by = 0.$$

The intersection between  $\mathbf{P}$  and such a line is given by the roots of the equation

$$f(t) = q(x(t), y(t), w(t)) = \sum_{i=0}^n f_i B_i^n(t) = 0$$

where

$$f_i = ax_i + by_i.$$

In the non-singular case  $k = 1$ , we have  $f_0 = 0$ . The tangent line has second-order contact with  $\mathbf{P}$ , and is therefore the line for which  $f_1 = ax_1 + by_1 = 0$ , which is the line  $\mathbf{P}_0\mathbf{P}_1$ . But if  $\mathbf{P}$  is singular, we have  $f_0 = \dots = f_{k-1} = 0$  for all values of  $a$  and  $b$ . The tangent line is the one that has highest intersection multiplicity, which is the one for which  $f_k = a_k x + b_k y = 0$ . This is the line  $\mathbf{P}_0\mathbf{P}_k$ .  $\square$

**Theorem 2.** For a singular Bézier curve  $\mathbf{P}$  under the conditions in (8), the limit curvature at  $\mathbf{P}(0)$  is  $\infty$  unless  $\mathbf{P}_{k+1}, \dots, \mathbf{P}_{2k-1}$  are collinear with  $\mathbf{P}_0\mathbf{P}_k$  and  $\omega_{2k} > 0$ ; then the limit curvature is

$$\kappa = \frac{2\binom{n}{2k}}{\binom{n}{k}^2} \frac{\omega_0 \omega_{2k}}{\omega_k^2} \frac{h}{a^2} \tag{9}$$

where  $a$  and  $h$  are the distances shown in Fig. 6. In the non-degenerate case  $k = 1$ , (9) reduces to (7) as expected.

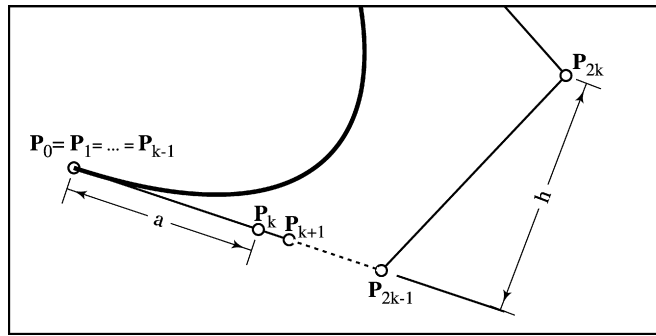


Fig. 6. Conditions for finite limit curvature at singular endpoint.

**Proof.** Set  $\mathbf{P}_k = (x_k, 0)$ ,  $x_k \neq 0$ , so that the tangent line is the  $x$ -axis. The intersection between  $\mathbf{P}$  and parabola  $\mathbf{Q}$  (3) is given by (4) where the  $f_i$  are given by (5). Since  $x_0 = \dots = x_{k-1} = 0$  and  $y_0 = \dots = y_k = 0$ , we have  $f_0 = \dots = f_k = 0$  for all choices of  $c_1$  and  $c_2$ . The *osculating* parabola is the one with largest intersection multiplicity. The osculating parabola must cause  $f_{k+1} = 0$ . From (5),

$$f_{k+1} = -\frac{\binom{n}{k+1}c_2\omega_0\omega_{k+1}y_{k+1}}{\binom{2n}{k+1}}$$

which vanishes if  $c_2 = 0$  or  $y_{k+1} = 0$ . If  $c_2 = 0$ , the curvature is  $\infty$ . Indeed, as illustrated in Fig. 1(a), this is the correct limit curvature if  $y_{k+1} \neq 0$ .

We next consider the special case  $y_{k+1} = 0$ , which causes  $f_{k+1} \equiv 0$  and the osculating parabola is the one that causes  $f_{k+2} = 0$ . However, this only happens if  $c_2 = 0$  (which again implies infinite curvature) or  $y_{k+2} = 0$ . So we set  $y_{k+2} = 0$  and check for conditions under which  $f_{k+3} = 0$ . Continuing this process, we eventually find that a finite curvature exists only for curves for which

$$y_0 = \dots = y_{2k-1} = 0 \quad \text{and} \quad x_k \neq 0. \tag{10}$$

In this case,  $f_0 = \dots = f_{2k-1} = 0$  and

$$f_{2k} = c_1 \frac{\binom{n}{k}^2}{\binom{2n}{2k}} \omega_k^2 x_k^2 - c_2 \frac{\binom{n}{0} \binom{n}{2k}}{\binom{2n}{2k}} \omega_0 \omega_{2k} y_{2k}. \tag{11}$$

The ratio  $c_1/c_2$  that makes (11) vanish (and thus defines the osculating parabola) is

$$\frac{c_1}{c_2} = \frac{\kappa}{2} = \frac{\binom{n}{2k}}{\binom{n}{k}^2} \frac{\omega_0 \omega_{2k}}{\omega_k^2} \frac{y_{2k}}{x_k^2}.$$

Consequently, the limit curvature of a singular curve (2) subject to (8) and (10) is

$$\kappa = 2 \frac{\binom{n}{2k}}{\binom{n}{k}^2} \frac{\omega_0 \omega_{2k}}{\omega_k^2} \frac{y_{2k}}{x_k^2}. \tag{12}$$

For our choice of coordinate system,  $x_k = a$  and  $y_{2k} = h$ .  $\square$

Theorems 1 and 2 can also be proven using L'Hospital's rule or by analyzing the limit of  $\kappa(t)$  as  $t \rightarrow 0$ , although the proofs are more complicated.

### 3.1. Three-dimensional curves

For singular rational Bézier curves in  $\mathbb{R}^3$ , Theorem 3 follows trivially from the  $\mathbb{R}^2$  case. Theorem 4 restates Eq. (9) by replacing  $a$  and  $h$  with vector expressions. Theorem 5 follows directly from the definition of Frenet frame.

**Theorem 3.** A Bézier curve in  $\mathbb{R}^3$  subject to (8) has tangent vector  $\mathbf{P}_k - \mathbf{P}_0$  at  $t = 0$ .

**Theorem 4.** A Bézier curve in  $\mathbb{R}^3$  subject to (8) has finite limit curvature at  $t = 0$  if and only if each control point  $\mathbf{P}_{k+1}, \dots, \mathbf{P}_{2k-1}$  is collinear with  $\mathbf{P}_0 - \mathbf{P}_k$ , in which case

$$\kappa(0) = \frac{2 \binom{n}{2k} \omega_0 \omega_{2k} \|(\mathbf{P}_k - \mathbf{P}_0) \times (\mathbf{P}_{2k} - \mathbf{P}_0)\|}{\binom{n}{k}^2 \omega_k^2 \|(\mathbf{P}_k - \mathbf{P}_0)\|^3}. \tag{13}$$

**Theorem 5.** If  $(\mathbf{P}_k - \mathbf{P}_0) \times (\mathbf{P}_{2k} - \mathbf{P}_0) \neq 0$ , the Frenet frame for a rational Bézier curve in  $\mathbb{R}^3$  subject to (8) is:

- (1) the tangent vector is  $\mathbf{T} = \mathbf{P}_k - \mathbf{P}_0$ ;
- (2) the bi-normal vector is  $(\mathbf{P}_k - \mathbf{P}_0) \times (\mathbf{P}_{2k} - \mathbf{P}_0)$ ;
- (3) the normal vector is  $\mathbf{N} = ((\mathbf{P}_k - \mathbf{P}_0) \times (\mathbf{P}_{2k} - \mathbf{P}_0)) \times (\mathbf{P}_k - \mathbf{P}_0)$ .

**Corollary 6.** The osculating plane for a rational Bézier curve in  $\mathbb{R}^3$  subject to (8) is spanned by  $\mathbf{T}$  and  $\mathbf{N}$  and is the plane containing  $\mathbf{P}_0$  that has the largest intersection multiplicity with  $\mathbf{P}$  at  $t = 0$ .

### 3.2. Zero weights

We have required  $\omega_0, \omega_k, \omega_{2k} > 0$ . If initially any  $\omega_i = 0$ , the order-of-contact method of computing curvature can still be used after we first find an equivalent curve for which all  $\omega_i > 0$  as follows. If  $\omega_0 = \dots = \omega_{m-1} = 0$ ,  $\mathbf{P}(t)$  can be replaced with

$$\hat{\mathbf{P}}(t) = \frac{\sum_{i=0}^{n-m} \hat{\omega}_i \hat{\mathbf{P}}_i B_i^{n-m}(t)}{\sum_{i=0}^{n-m} \hat{\omega}_i B_i^{n-m}(t)} \quad \text{where } \hat{\mathbf{P}}_i = \mathbf{P}_{i+m}, \quad \hat{\omega}_i = \frac{\binom{n}{i+m}}{\binom{n}{i}} \omega_{i+m}.$$

The case  $\omega_{n-m+1} = \dots = \omega_n = 0$  can be dealt with in similar fashion. Any other zero weights can be eliminated through degree elevation.

## 4. Singular surface patches

We consider the rational tensor-product Bézier surface

$$\tilde{\mathbf{C}}(\tilde{u}, \tilde{v}) = \frac{(\tilde{x}(\tilde{u}, \tilde{v}), \tilde{y}(\tilde{u}, \tilde{v}), \tilde{z}(\tilde{u}, \tilde{v}))}{\tilde{\omega}(\tilde{u}, \tilde{v})} = \frac{\sum_{i=0}^m \sum_{j=0}^n \tilde{\omega}_{ij} \tilde{\mathbf{C}}_{ij} B_i^m(\tilde{u}) B_j^n(\tilde{v})}{\sum_{i=0}^m \sum_{j=0}^n \tilde{\omega}_{ij} B_i^m(\tilde{u}) B_j^n(\tilde{v})}. \tag{14}$$

We will use the form

$$\mathbf{C}(u, v) = (x(u, v), y(u, v), z(u, v), w(u, v)) = \sum_{i=0}^m \sum_{j=0}^n (x_{ij}, y_{ij}, z_{ij}, w_{ij}) u^i v^j \tag{15}$$

which is equivalent to (14) under the substitutions  $w_{ij} = \binom{m}{i} \binom{n}{j} \tilde{\omega}_{ij}$ ,  $\mathbf{C}_{ij} = (x_{ij}, y_{ij}, z_{ij}) = \binom{m}{i} \binom{n}{j} \tilde{\omega}_{ij} \tilde{\mathbf{C}}_{ij}$ ,  $u = \frac{\tilde{u}}{1-\tilde{u}}$ , and  $v = \frac{\tilde{v}}{1-\tilde{v}}$  and the reparametrization  $\tilde{x}(\tilde{u}, \tilde{v}) = x(u, v) * (1 - \tilde{u})^m (1 - \tilde{v})^n$ , etc. We translate the surface so that  $\tilde{\mathbf{C}}_{0,0} = \mathbf{C}_{0,0} = (0, 0, 0)$ .

Our discussion makes heavy use of the set

$$\Gamma_{i_0, j_0} = \left\{ \mathbf{P}(t) = \mathbf{C}(u(t), v(t)) \mid u(t) = \sum_{i=i_0}^{\infty} u_i t^i, v(t) = \sum_{j=j_0}^{\infty} v_j t^j \right\} \tag{16}$$

with  $u_{i_0}, v_{j_0}$  not both zero, and where

$$\mathbf{P}(t) = \sum_{i=0}^{\infty} (\mathbf{P}_i, w_i) t^i = \sum_{i=0}^{\infty} (x_i, y_i, z_i, w_i) t^i. \tag{17}$$

We are particularly interested in  $\Gamma_{i_0, j_0}$  that represents the set of all analytic curves  $(u(t), v(t))$  whose images pass through  $\mathbf{C}_{00}$ . For almost all singularities,  $\Gamma_{1,1}$  meets this requirement. Exceptions are that for a singularity for which  $\mathbf{C}(u, 0) \equiv \mathbf{C}(0, 0)$ ,  $u \in R$ , we must use  $\Gamma_{0,1}$  and for a singularity for which  $\mathbf{C}(0, v) \equiv \mathbf{C}(0, 0)$ ,  $v \in R$ , we must use  $\Gamma_{1,0}$ . In the remainder of the paper,  $\Gamma = \Gamma_{1,1}$ . Only in Section 7.2.1 will we use  $\Gamma_{0,1}$ .

We enforce  $w_0 = \omega_{00} \neq 0$  to avoid a base point; the method of eliminating zero weights in Section 3.2 does not extend to surfaces.

**Definition 7.** Depending on its argument, the function  $\mathcal{L}$  means:

1.  $\mathcal{L}(\mathbf{P}) = k$ , where  $\mathbf{P} \in \Gamma$ ,  $\mathbf{P}_0 = \dots = \mathbf{P}_{k-1} = (0, 0, 0) \neq \mathbf{P}_k$ .
2.  $\mathcal{L}(\mathbf{C}(u, v))$  is the smallest sum  $i + j$  for which there exists a  $\mathbf{C}_{ij} \neq (0, 0, 0)$ .
3. If  $\mathcal{S}$  is a set of polynomials,  $\mathcal{L}(\mathcal{S}) = \min\{\mathcal{L}(\mathbf{P}) \mid \mathbf{P} \in \mathcal{S}\}$ . For example,  $\mathcal{L}(\Gamma) = \min\{\mathcal{L}(\mathbf{P}) \mid \mathbf{P} \in \Gamma\}$ .

**Definition 8.**  $\mathbf{C}$  is singular at  $\mathbf{C}(0, 0)$  if there exists a curve  $\mathbf{P} \in \Gamma$  for which  $\mathcal{L}(\mathbf{P}) > 1$ .

**Definition 9.** An anomalous curve is any  $\mathbf{P} \in \Gamma$  for which  $\mathcal{L}(\mathbf{P}) > \mathcal{L}(\Gamma)$ .

A curve  $\mathbf{P} \in \Gamma$  is anomalous if and only if  $\mathbf{P}_k = (0, 0, 0)$  where  $k = \mathcal{L}(\Gamma)$ . Since  $\mathbf{P} = \mathbf{C}(u(t), v(t))$ , and  $\mathbf{C}_{ij} = (0, 0, 0)$  for all  $i + j < k$ , an anomalous curve occurs only when:

$$\mathbf{P}_k = (x_k(u_1, v_1), y_k(u_1, v_1), z_k(u_1, v_1)) = \sum_{i+j=k} \mathbf{C}_{ij} u_1^i v_1^j = (0, 0, 0). \tag{18}$$

Each homogeneous polynomial equation  $x_k(u_1, v_1) = 0$ ,  $y_k(u_1, v_1) = 0$ ,  $z_k(u_1, v_1) = 0$  has  $k$  roots  $u_1 : v_1$ , so (18) is satisfied only when all three polynomials have one or more roots in common; this will not happen if the  $\mathbf{C}_{ij}$ ,  $i + j = k$ , are in general position. The difference  $\mathcal{L}(\mathbf{P}) - \mathcal{L}(\Gamma)$  is the order of the anomaly. We will call each root of (18) an anomalous direction, because each ratio  $u_1 : v_1$  defines a tangent direction in  $(u, v)$  space. The maximum number of anomalous directions is  $k$ , which is realized only if the triples  $\mathbf{C}_{ij}$ ,  $i + j = k$ , are scales of each other.

4.1. Examples of singularities and anomalous curves

1. The only class of singularities which have no anomalous curves are those for which  $\mathbf{C}_{ij} = (0, 0, 0)$ ,  $1 \leq i + j < k$ , and for which  $\sum_{i+j=k} \mathbf{C}_{ij} u_1^i v_1^j \neq (0, 0, 0)$  for any non-trivial  $u_1, v_1$ . This is the case if all  $\mathbf{C}_{ij}$ ,  $i + j = k$ , are in general position.
2. The surface for which  $\mathbf{C}_{00} = (0, 0, 0)$  and  $\mathbf{C}_{10} = -\alpha \mathbf{C}_{01} \neq (0, 0, 0)$  is singular even though  $\mathcal{L}(\mathbf{C}(u, v)) = 1$ , because there is an anomalous curve at  $u_1 : v_1 = \alpha : 1$ . A generic  $\mathbf{P} \in \Gamma$  for this surface has coefficient  $\mathbf{P}_1 = (u_1 - \alpha v_1) \mathbf{C}_{10}$ , so all non-anomalous  $\mathbf{P} \in \Gamma$  have an endpoint tangent vector parallel to  $\mathbf{C}_{10} - (0, 0, 0)$ . Anomalous curves have coefficient  $\mathbf{P}_2 = (u_2 - \alpha v_2) \mathbf{C}_{10} + u_1^2 \mathbf{C}_{20} + 2u_1 v_1 \mathbf{C}_{11} + v_1^2 \mathbf{C}_{02}$ .
3. For a surface with  $\mathbf{C}_{10} = \mathbf{C}_{00} = (0, 0, 0) \neq \mathbf{C}_{01}$ , a family of anomalous curves exists with  $v_1 = 0$ . For each anomalous curve,  $\mathbf{P}_0 = \mathbf{P}_1 = (0, 0, 0)$  and

$$\mathbf{P}_2 = \mathbf{C}_{20} u_1^2 + \mathbf{C}_{01} v_2, \quad \mathbf{P}_3 = \mathbf{C}_{30} u_1^3 + 2\mathbf{C}_{20} u_1 u_2 + \mathbf{C}_{11} u_1 v_2 + \mathbf{C}_{01} v_3.$$

The curvature of this specific singular surface is addressed in Wolter and Tuohy (1991). A higher-order anomaly can be created if  $\mathbf{C}_{01} = -\alpha \mathbf{C}_{20}$  because then  $\mathbf{P}_2 = (0, 0, 0)$  if  $\frac{u_1^2}{v_2} = \alpha$  – this case is not allowed in Wolter and Tuohy (1991). This example illustrates the fact that anomalous curves can be “nested” in the sense that one family of anomalous curves can include higher-order anomalous curves.

4. The surface for which  $\mathbf{C}_{00} = \mathbf{C}_{10} = \mathbf{C}_{01} = (0, 0, 0)$  is singular, with  $\mathcal{L}(\Gamma) = \mathcal{L}(\mathbf{C}(u, v)) = 2$ . A generic  $\mathbf{P} \in \Gamma$  for this surface has coefficient  $\mathbf{P}_2 = \mathbf{C}_{20} u_1^2 + \mathbf{C}_{11} u_1 v_1 + \mathbf{C}_{02} v_1^2$  and if  $\mathbf{C}_{20}$ ,  $\mathbf{C}_{11}$ , and  $\mathbf{C}_{02}$  are in general position, this case is described in example (1) and has no anomalous curves. If, however, we have  $\mathbf{C}_{20} = (2, 4, 0)$ ,  $\mathbf{C}_{11} = (3, 4, 0)$ ,  $\mathbf{C}_{02} = (-2, -3, 0)$ , then  $\mathbf{P}_2 = (0, 0, 0)$  for all curves  $\mathbf{P} \in \Gamma$  for which  $u_1 : v_1 = 1 : 2$ . Such curves are anomalous, with  $\mathcal{L}(\mathbf{P}) > 2$ .

5. Tangent plane at a singular corner

Denote by  $L(\mathbf{P})$  the coefficient of the leading non-zero term for a curve  $\mathbf{P} \in \Gamma$ , that is,  $L(\mathbf{P}) = \mathbf{P}_k$  where  $k = \mathcal{L}(\mathbf{P})$ . Define

$$T = \{L(\mathbf{P}) - \mathbf{P}_0 \mid \mathbf{P} \in \Gamma\}. \tag{19}$$

**Theorem 10.** If  $T$  spans a vector space with dimension 2, a tangent plane exists.

**Proof.**  $L(\mathbf{P}) - \mathbf{P}_0$  defines the tangent direction of each  $\mathbf{P} \in \Gamma$ . Thus,  $T$  is the set of tangent directions for all  $\mathbf{P} \in \Gamma$  and hence is the tangent space for the surface at  $\mathbf{C}(0, 0)$ . If  $T$  spans a vector space of dimension 2, the tangent space lies in a plane.  $\square$

**Corollary 11.** At the origin, all non-anomalous curves  $\mathbf{P} \in \Gamma$  have tangent vectors that are linear combinations of the vectors  $\mathbf{C}_{ij} - \mathbf{C}_{00}$ ,  $i + j = k = \mathcal{L}(\Gamma)$ .

**Proof.** For a non-anomalous curve,  $\mathbf{P}_k \neq (0, 0, 0)$  and  $\mathbf{P}_0 = \mathbf{C}_{00}$ . From (18),  $\mathbf{P}_k$  is a linear combination of  $\mathbf{C}_{ij}$ ,  $i + j = k$ . Therefore, the tangent vector  $\mathbf{P}_k - \mathbf{P}_0$  is a linear combinations of the vectors  $\mathbf{C}_{ij} - \mathbf{C}_{00}$ ,  $i + j = k$ .  $\square$

**Corollary 12.** Sufficient condition for the existence of a tangent plane at the point  $\mathbf{C}(0, 0)$  is that  $\Gamma$  contains no anomalous curves, and that the vectors  $\mathbf{C}_{ij} - \mathbf{C}_{00}$ ,  $i + j = k = \mathcal{L}(\Gamma)$ , span a vector space with dimension 2.

**Proof.** For all  $\mathbf{P} \in \Gamma$ ,  $L(\mathbf{P})$  is a linear combination of  $\mathbf{C}_{ij}$ ,  $i + j = k$ . Therefore, if all vectors  $\mathbf{C}_{ij} - \mathbf{C}_{00}$ ,  $i + j = k$ , span a vector space with dimension 2, so must  $T$ .  $\square$

If a surface has anomalous curves, additional constraints are needed to assure the existence of a tangent plane.

**6. Gaussian and mean curvature at a singular corner**

Define

$$F = \{ f(x, y, z, w) = ax^2 + bxy + cy^2 - dzw \mid a, b, c, d \in \mathbb{R} \} \tag{20}$$

where, for each  $f \in F$ ,  $f = 0$  is a paraboloid that has a tangent plane  $z = 0$  at the origin. For each  $f \in F$  and  $\mathbf{P} \in \Gamma$ , the composition

$$g(t) = f \circ \mathbf{P} = f(x(t), y(t), z(t), w(t))$$

is a polynomial whose roots are the values of  $t$  at which  $\mathbf{P}$  intersects the paraboloid  $f = 0$ . We will say that a paraboloid osculates with  $\mathbf{P} \in \Gamma$  if  $\mathcal{L}(f \circ \mathbf{P}) > \mathcal{L}(F \circ \mathbf{P})$  where  $F \circ \mathbf{P} = \{f \circ \mathbf{P} \mid f \in F\}$ . An osculating paraboloid osculates with all  $\mathbf{P} \in \Gamma$ .

Assume that  $\mathbf{C}$  has a tangent plane  $z = 0$  at  $\mathbf{C}(0, 0) = (0, 0, 0)$ . If an osculating paraboloid  $ax^2 + bxy + cy^2 - dzw = 0$  exists, Theorem 14 shows that its curvatures at  $(0, 0, 0)$  are the limit curvatures of  $\mathbf{C}$ . Specifically, Gaussian curvature is

$$K = K_1 K_2 = \frac{4ac - b^2}{d^2}, \tag{21}$$

mean curvature is

$$H = \frac{K_1 + K_2}{2} = \frac{a + c}{d}, \tag{22}$$

principle curvatures are

$$K_1, K_2 = \frac{a + c \pm \sqrt{b^2 + (a - c)^2}}{d},$$

and the principal planes are

$$[c - a + \sqrt{b^2 + (a - c)^2}]x - by = 0 \quad \text{and} \quad [-c + a + \sqrt{b^2 + (a - c)^2}]x + by = 0.$$

The proof of Theorem 14 focuses on normal curvatures. A normal plane  $\mathbf{N}$  through a singular point of a surface  $\mathbf{C}$  will generally intersect  $\mathbf{C}$  in a curve that has two or more branches that are tangent to each other, as suggested by Fig. 4(b).

**Lemma 13.** Given a singular surface  $\mathbf{C}(u, v)$  (15) that has a tangent plane  $z = 0$ . For each normal plane  $\mathbf{N}$ , each branch of  $\mathbf{N} \cap \mathbf{C}$  is intersected by a curve in  $\Gamma$  with intersection multiplicity  $\geq r$  at  $\mathbf{C}(0, 0)$ , where  $r$  is any integer.

**Proof.** Let  $\mathbf{N}$  be the plane  $ax + by = 0$ . The curve  $\mathbf{N} \cap \mathbf{C}$ , given by

$$f(u, v) = a * x(u, v) + b * y(u, v) = \sum_{i=0}^m \sum_{j=0}^n \alpha_{ij} u^i v^j = 0, \quad \text{where } \alpha_{ij} = ax_{ij} + by_{ij},$$

can have several branches (e.g., Fig. 4(b)). For each branch, we prove the existence of  $(u(t), v(t))$  (16) such that the first  $r$  coefficients of

$$g(t) = f(u(t), v(t)) = \sum_{i=0}^{\infty} g_i t^i$$

vanish. Letting  $k = \mathcal{L}(f(u, v))$ , we have  $g_0 = \dots = g_{k-1} = 0$  and

$$g_k = \sum_{i+j=k} \alpha_{ij} u_1^i v_1^j = 0. \tag{23}$$

There is one real solution  $u_1 : v_1$  to (23) for each real branch of  $\mathbf{N} \cap \mathbf{C}$ . Fixing  $u_1 : v_1$  to be one of those roots, we find that the coefficient  $g_{k+1}$  is linear in  $u_2$  and  $v_2$  and does not involve  $u_\beta, v_\beta, \beta > 2$ , so we can solve  $u_2 : v_2$  to cause  $g_{k+1} = 0$ . Likewise, the coefficient  $g_{k+\mu}$  is linear in  $u_{\mu+1}$  and  $v_{\mu+1}$  and does not involve  $u_\beta, v_\beta, \beta > \mu + 1$ , so we can systematically zero out  $g_k, \dots, g_r$ .  $\square$



**Theorem 14.** *If a singular surface  $\mathbf{C}$  has an osculating paraboloid  $\mathcal{P}$ , the limit Gaussian and mean curvatures of  $\mathbf{C}$  are equal to the Gaussian and mean curvatures of  $\mathcal{P}$ .*

**Proof.** We show that, for any normal plane  $\mathbf{N}$  through  $(0, 0, 0)$ , the limit curvature of  $\mathbf{N} \cap \mathbf{C}$  is equal to the curvature of  $\mathbf{N} \cap \mathcal{P}$ . Let  $\mathcal{C} \in \Gamma$  be a curve that intersects  $\mathbf{N} \cap \mathbf{C}$  with multiplicity  $2k + 1$  where  $k = \mathcal{L}(\mathcal{C})$ . Lemma 13 assures the existence of  $\mathcal{C}$ . By the definition of osculating paraboloid,  $\mathcal{C}$  osculates with  $\mathcal{P}$ . If we express  $\mathcal{C}$  in Bézier form, its first  $k$  control points lie at the origin, and its first  $2k + 1$  control points lie on  $\mathbf{N}$ .  $\mathcal{C}$  thus also osculates with  $\mathbf{N} \cap \mathcal{P}$  and therefore has the same limit curvature as  $\mathbf{N} \cap \mathcal{P}$ .  $\square$

## 7. Examples

Theorem 14 provides a general mechanism for analyzing curvature. The conditions under which an osculating paraboloid exists can be expressed in straightforward algebraic terms. This section presents several examples.

### 7.1. Curvature when there are no anomalous curves

In this section we discuss the curvature of surfaces that have no anomalous curves and  $k = \mathcal{L}(\mathbf{P})$ . We assure a tangent plane of  $z = 0$  by setting  $\mathbf{C}_{ij} = (0, 0, 0)$ ,  $i + j < k$ , and  $\mathbf{C}_{ij} = (x_{ij}, y_{ij}, 0)$ ,  $i + j = k$ .

#### 7.1.1. Curvature at a non-singular point

We begin by showing how the approach works in the non-singular case,  $k = 1$  and  $z_{10} = z_{01} = 0$ . Thus,  $g = f \circ \mathbf{P} = \sum_{i=0}^p g_i t^i$  has  $g_0 = g_1 = 0$  and

$$g_2 = (ax_{10}^2 + bx_{10}y_{10} + cy_{10}^2 - dw_{00}z_{20})u_1^2 + (2ax_{10}x_{01} + b(x_{10}y_{01} + y_{10}x_{01}) + 2cy_{10}y_{01}u_1v_1 - dw_{00}z_{11})u_1v_1 + (ax_{01}^2 + bx_{01}y_{01} + cy_{01}^2 - dw_{00}z_{02})v_1^2. \quad (24)$$

Therefore,  $\mathcal{L}(F \circ \Gamma) = 2$  and the osculating paraboloid  $f = 0$  ( $f \in F$ ) will cause  $\mathcal{L}(f \circ \Gamma) > 2$ . Necessary and sufficient condition for this to happen is for  $g_2$  to vanish for all values of  $u_1$  and  $v_1$  (other than  $u_1 = v_1 = 0$ ). This requires the coefficients of  $u_1^2$ ,  $u_1v_1$ , and  $v_1^2$  in (24) to all vanish, which will happen if and only if the following three linear equations are satisfied:

$$\begin{bmatrix} x_{10}^2 & x_{10}y_{10} & y_{10}^2 & -w_{00}z_{20} \\ 2x_{10}x_{01} & x_{10}y_{01} + y_{10}x_{01} & 2y_{10}y_{01} & -w_{00}z_{11} \\ x_{01}^2 & x_{01}y_{01} & y_{01}^2 & -w_{00}z_{02} \end{bmatrix} \begin{bmatrix} a \\ b \\ c \\ d \end{bmatrix} = \begin{bmatrix} 0 \\ 0 \\ 0 \end{bmatrix}. \quad (25)$$

The solutions for this linear system are scales of

$$\begin{aligned} a &= \omega_{00}z_{02}y_{10}^2 - y_{01}\omega_{00}z_{11}y_{10} + y_{01}^2\omega_{00}z_{20}, \\ b &= -2x_{01}y_{01}\omega_{00}z_{20} + y_{10}x_{01}\omega_{00}z_{11} + x_{10}y_{01}\omega_{00}z_{11} - 2x_{10}y_{10}\omega_{00}z_{02}, \\ c &= \omega_{00}z_{02}x_{10}^2 - x_{01}\omega_{00}z_{11}x_{10} + x_{01}^2\omega_{00}z_{20}, \\ d &= (y_{10}x_{01} - x_{10}y_{01})^2. \end{aligned}$$

The Gaussian curvature (21) for this osculating paraboloid is  $K = (4ac - b^2)/d^2$ , or

$$K = \frac{4w_{00}^2z_{20}z_{02} - w_{00}^2z_{11}^2}{(y_{10}x_{01} - x_{10}y_{01})^2} = \frac{\tilde{w}_{00}^2}{\tilde{w}_{10}^2\tilde{w}_{01}^2} \frac{\binom{m-1}{m} \binom{n-1}{n} \tilde{w}_{20}\tilde{w}_{02}\tilde{z}_{20}\tilde{z}_{02} - \tilde{w}_{11}^2\tilde{z}_{11}^2}{(\tilde{y}_{10}\tilde{x}_{01} - \tilde{x}_{10}\tilde{y}_{01})^2}. \quad (26)$$

Mean curvature can be found from (22). These formulae are equivalent to those derived in Zheng and Sederberg (2003) using differential geometry.

#### 7.1.2. Curvature at a singular non-anomalous point

Again assuring a  $z = 0$  tangent plane by imposing  $\mathbf{C}_{ij} = (0, 0, 0)$ ,  $i + j < k$ , and  $\mathbf{C}_{ij} = (x_{ij}, y_{ij}, 0)$ ,  $i + j = k$ , for the singular case ( $k > 1$ ) we have

$$g_{k+1} = d\omega_{00} \sum_{i+j=k+1} z_{ij}u_1^i v_1^j.$$

If any  $z_{ij} \neq 0$ ,  $i + j = k + 1$ , we can only have  $g_{k+1} = 0$  if  $d = 0$ , which implies infinite curvatures. This result is consistent with the curve case. As in the curve case, we can achieve finite curvature only if we force  $z_{ij} = 0$ ,  $i + j < 2k$ . In this case,  $\mathcal{L}(F \circ \Gamma) = 2k$ , and

$$g_{2k} = \sum_{i=0}^{2k} \left[ \sum_{\substack{j_1+k_1=i \\ j_1+j_2=k \\ k_1+k_2=k}} [ax_{j_1j_2}x_{k_1k_2} + bx_{j_1j_2}y_{k_1k_2} + cy_{j_1j_2}y_{k_1k_2}] - dw_{00}z_{i,2k-i} \right] u_1^i v_1^{2k-i}. \tag{27}$$

The osculating paraboloid will force  $g_{2k} = 0$  for all  $u_1, v_1$ .

We first consider the case  $k = 2$  and  $z_{ij} = 0, i + j < 4$ , for which the lowest-degree non-zero term of  $g$  is  $g_4$ . Specializing (27) to  $k = 2$ ,

$$g_4 = (ax_{20}^2 + bx_{20}y_{20} + cy_{20}^2 - dw_{00}z_{40})u_1^4 + (2ax_{20}x_{11} + b(x_{20}y_{11} + y_{20}x_{11}) + 2cy_{20}y_{11} - dw_{00}z_{31})u_1^3v_1 + (a(x_{11}^2 + 2x_{02}x_{20}) + b(x_{02}y_{20} + x_{11}y_{11} + x_{20}y_{02}) + c(y_{11}^2 + 2y_{02}y_{20}) - dw_{00}z_{22})u_1^2v_1^2 + (2ax_{02}x_{11} + b(x_{02}y_{11} + y_{02}x_{11}) + 2cy_{02}y_{11} - dw_{00}z_{13})u_1v_1^3 + (2ax_{02}x_{02} + bx_{02}y_{02} + cy_{02}^2 - dw_{00}z_{04})v_1^4. \tag{28}$$

An osculating paraboloid exists if  $g_4 \equiv 0$  for all  $u_1, v_1$ , which requires a solution to the linear system:

$$\begin{bmatrix} x_{20}^2 & x_{20}y_{20} & y_{20}^2 & z_{40} \\ 2x_{20}x_{11} & x_{20}y_{11} + y_{20}x_{11} & 2y_{20}y_{11} & z_{31} \\ x_{11}^2 + 2x_{02}x_{20} & x_{02}y_{20} + x_{11}y_{11} + x_{20}y_{02} & y_{11}^2 + 2y_{02}y_{20} & z_{22} \\ 2x_{02}x_{11} & x_{02}y_{11} + y_{02}x_{11} & 2y_{02}y_{11} & z_{13} \\ x_{02}^2 & x_{02}y_{02} & y_{02}^2 & z_{04} \end{bmatrix} \begin{bmatrix} a \\ b \\ c \\ -w_{00}d \end{bmatrix} = 0 \tag{29}$$

or  $[V_1 \ V_2 \ V_3 \ Z][A] = [0]$ . A solution exists for (29) only if the rank of the matrix is three. This can be achieved, for example, by fixing the  $x_{ij}$  and  $y_{ij}$  variables in the first three columns, selecting values for  $a, b, c$ , and  $d$ , then solving

$$Z = (aV_1 + bV_2 + cV_3)/\omega_{00}d. \tag{30}$$

The Gaussian and mean curvatures can be computed using (21) and (22). For general values of  $k$ , the matrix in (29) will have  $2k + 1$  rows.

7.2. Curvature in the presence of anomalous curves

We explore the complications introduced by anomalous curves using the simple case where  $C_{10} = C_{00} = (0, 0, 0) \neq C_{01}$ , in which a family of anomalous curves exists with  $v_1 = 0$ . All anomalous curves  $P \in \Gamma$  have coefficients  $P_0 = P_1 = (0, 0, 0)$  and

$$P_2 = C_{20}u_1^2 + C_{01}v_2.$$

Thus, necessary and sufficient conditions for a tangent plane of  $z = 0$  are that the  $z$  coordinates of  $C_{01}$  and  $C_{20}$  are zero, and  $C_{00}, C_{01}$  and  $C_{20}$  are distinct and non-collinear. This assures that  $T$  spans a vector space of dimension two.

To determine the existence of an osculating paraboloid, start with (25) which gives conditions for all non-anomalous curves on this surface to osculate with a paraboloid. Since in our current case  $C_{10} = (0, 0, 0)$ , the top row of the matrix in (25) is identically zero and can be removed. Additional linear constraints must now be added that will force all anomalous curves to osculate with the paraboloid. Letting  $g = f \circ P$  where  $P$  represents all anomalous curves,  $g_0 = g_1 = g_2 = 0$ . Osculation occurs if  $g_3 = 0$ , but in this case,  $g_3 = -dw_{00}z_{11}u_1v_2 - dw_{00}z_{30}u_1^3$ , for which the osculating paraboloid has  $d = 0$ , which implies infinite curvature. Instead, we proceed as in previous cases and set  $z_{11} = z_{30} = 0$ . Now the lowest-degree non-zero term has coefficient

$$g_4 = (ax_{01}^2 + bx_{01}y_{01} + cy_{01}^2 - dw_{00}z_{02})v_2^2 + (2ax_{01}x_{20} + b(x_{20}y_{01} + x_{01}y_{20}) + 2cy_{01}y_{20} - dw_{00}z_{21})u_1^2v_2 + (ax_{20}^2 + bx_{20}y_{20} + cy_{20}^2 - dw_{00}z_{40})u_1^4. \tag{31}$$

We seek values of  $a, b, c, d$  that will force  $g_4 = 0$  for all values of  $u_1$  and  $v_2$ . We also require that those same values of  $a, b, c, d$  will satisfy the linear system (25), excluding the top row of the matrix. This results in a matrix with five rows, two of which are identical. After removing the redundant row, we obtain (32), whose top two rows come from (25) and whose bottom three rows come from (31):

$$\begin{bmatrix} 2x_{10}x_{01} & x_{10}y_{01} + y_{10}x_{01} & 2y_{10}y_{01} & -w_{00}z_{11} \\ x_{01}^2 & x_{01}y_{01} & y_{01}^2 & -w_{00}z_{02} \\ 2x_{01}x_{20} & x_{20}y_{01} + x_{01}y_{20} & 2y_{01}y_{20} & -w_{00}z_{21} \\ x_{20}^2 & x_{20}y_{20} & y_{20}^2 & -w_{00}z_{40} \end{bmatrix} \begin{bmatrix} a \\ b \\ c \\ d \end{bmatrix} = \begin{bmatrix} 0 \\ 0 \\ 0 \\ 0 \end{bmatrix}. \tag{32}$$

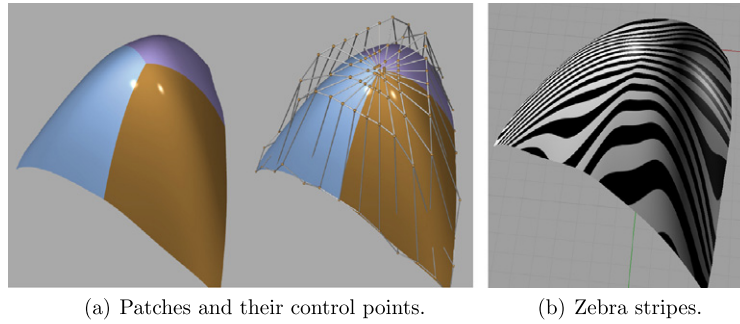


Fig. 7. Three Bézier patches that are  $C^2$  along their shared boundary curves and  $G^2$  at the extraordinary point.

The existence of an osculating paraboloid is assured when the matrix is rank three. A solution can be found using, for example, (30).

Generalizing from this example, we propose a three-step strategy for determining the existence of a finite Gaussian and mean limit curvature at a singular point that has anomalous curves.

- Step 1.** Set up a linear system, as in (29), that solves for paraboloid that osculates with all non-anomalous curves. This matrix will have  $2k + 1$  rows, where  $k = \mathcal{L}(\mathbf{C}(u, v))$ . Each anomalous direction will introduce a linear dependency into the linear system, allowing the removal of one row for each dependency.
- Step 2.** Add some additional rows to the matrix to force the paraboloid to osculate with each anomalous curve, following the example in (32).
- Step 3.** If the rank of the matrix is three, solve for  $a, b, c, d$  to obtain the osculating paraboloid, from which the Gaussian and mean limit curvatures can be computed using (21) and (22). If the rank is not three, no osculating paraboloid exists. Constraints can be imposed on the control points of the surface patch to force a rank of three and assure the existence of an osculating paraboloid.

7.2.1. Edge collapsing to a point

We now analyze when a bicubic patch with  $\mathbf{C}_{00} = \mathbf{C}_{10} = \mathbf{C}_{20} = \mathbf{C}_{30} = (0, 0, 0)$  has finite Gaussian and mean limit curvatures. Since  $\Gamma$  does not contain all analytic curves on  $\mathbf{C}$  passing through  $\mathbf{C}_{00}$ , we must use  $\Gamma_{0,1}$  (see (16)). Then

$$\mathbf{P}_1 = v_1 \mathbf{C}_{01} + u_0 v_1 \mathbf{C}_{11} + u_0^2 v_1 \mathbf{C}_{21} + u_0^3 v_1 \mathbf{C}_{31}.$$

As long as there are no  $(u_0, v_1)$  pairs for which  $\mathbf{P}_1 = (0, 0, 0)$ , this surface has no anomalous curves, and necessary and sufficient conditions for the existence of a tangent plane is that  $\tilde{\mathbf{C}}_{00}, \tilde{\mathbf{C}}_{01}, \tilde{\mathbf{C}}_{11}, \tilde{\mathbf{C}}_{21},$  and  $\tilde{\mathbf{C}}_{31}$  are all co-planar. To analyze curvature, let the tangent plane be  $z = 0$  by setting  $\mathbf{C}_{i,1} = (x_{i,1}, y_{i,1}, 0), i = 0, 1, 2, 3$ . Then  $F \circ \Gamma = \{f \circ \mathbf{P} \mid f \in F, \mathbf{P} \in \Gamma\}$  is a polynomial in  $t$  whose first two terms vanish, and for which the coefficient of  $t^2$  is of the form

$$\sum_{i=0}^6 r_i u_0^i v_1^2, \tag{33}$$

where the  $r_i$  are expressions in terms of  $a, b, c, d, x_{jk}, y_{jk}, z_{jk},$  and  $w_{jk}$ . The vanishing of (33) for all values of  $u_0$  and  $v_1$  requires all  $r_i$  to vanish. This can be represented in matrix form  $M[a, b, c, d]^T = 0$ , where each row of  $M$  is an  $r_i$ , and

$$M = \begin{bmatrix} x_{01}^2 & x_{01}y_{01} & y_{01}^2 & -w_{00}z_{02} \\ 2x_{01}x_{11} & x_{01}y_{01} + x_{11}y_{01} & 2y_{01}y_{11} & -w_{10}z_{02} \\ x_{11}^2 + 2x_{01}x_{21} & x_{11}y_{11} + x_{01}y_{21} + x_{21}y_{01} & 2y_{01}y_{21} + y_{11}^2 & -w_{00}z_{22} - w_{10}z_{12} \\ 2x_{21}x_{11} + 2x_{01}x_{31} & x_{01}y_{31} + x_{21}y_{11} + x_{11}y_{21} + x_{31}y_{01} & 2y_{01}y_{31} + 2y_{11}y_{21} & -w_{00}z_{32} - w_{10}z_{22} \\ x_{21}^2 + 2x_{11}x_{31} & x_{31}y_{11} + x_{21}y_{21} + x_{11}y_{31} & y_{21}^2 + 2y_{11}y_{31} & -w_{20}z_{22} - w_{10}z_{32} \\ 2x_{21}x_{31} & x_{31}y_{21} + x_{21}y_{31} & 2y_{21}y_{31} & -w_{20}z_{32} \\ x_{31}^2 & x_{31}y_{31} & y_{31}^2 & -w_{30}z_{32} \end{bmatrix}.$$

An osculating paraboloid exists if  $M$  is rank 3.

7.3. Example

Fig. 7 shows three Bézier patches of degree  $6 \times 6$  that are pairwise  $C^2$  along their shared boundary curves, and  $G^2$  at the extraordinary point.  $C^2$  continuity along all edges that meet at an extraordinary point can only be attained if  $\mathbf{P}_{ij} = \mathbf{P}_{00}, i, j = 0, 1, 2$ , which introduces a singularity.  $G^2$  at the singular extraordinary points is assured by forcing all three patches

to have the same osculating paraboloid, based on the results in Section 7.1.2. The smooth zebra stripes evidence curvature continuity.

## 8. Conclusion

This paper shows that, while the limit curvature at a generic singular point of a rational Bézier curve is infinite, in some cases the limit curvature at a singularity is finite. Necessary and sufficient conditions are presented for this to occur.

Surface singularities can have many different forms, and the paper introduces the notion of anomalous curves to characterize and deal with those singularities. This allows us to analyze limit curvature in algebraic form, yielding a general method for stating necessary and sufficient conditions for the existence of tangent plane and curvature, along with formulae for computing them. These results have application in strategies for creating  $G^2$  extraordinary points, such as in TURBS surfaces, and in cases where an edge of control points collapses to a point.

The paper has focused on singular point for which one or more directional derivatives vanish, and has not discussed base points, because for a generic base point, directional derivatives do not vanish. Each base point maps (“blows up”) to an entire curve, so while base points are not singular in the sense used in this paper, a curvature analysis of base points does require special handling. Base points occur in Gregory patches and curvature at the corner of a Gregory patch is analyzed in Hermann (1996). We can also have singular base points for which directional derivatives vanish; this could be a topic for future research, although it is not clear if there is a practical CAGD application for the study.

Another interesting question is how floating point error impacts the curvature of singular curves and surfaces. For example, finite curvature requires some Bézier control points to be collinear or co-planar, yet with floating point arithmetic, exact collinearity or co-planarity cannot be assured. What does such truncation error imply about the curvature?

## Acknowledgements

This paper benefited tremendously from the referees' very helpful criticism. The first author's work was in support of a grant from ONR (No. 00460374). The second author was supported by Natural Science Foundation of China (Nos. 60970150, 60933008), and Zhejiang Provincial Natural Science Foundation of China (No. Y1090416). The third author was supported by Startup Scientific Research Foundation of CAS and NSF of China (No. 6093148).

## References

- Bohl, H., Reif, U., 1997. Degenerate Bézier patches with continuous curvature. *Computer Aided Geometric Design* 14, 749–761.
- Bruce, J.W., Giblin, P.J., 1984. *Curves and Singularities*. Cambridge University Press.
- Do Carmo, M.P., 1976. *Differential Geometry of Curves and Surfaces*. Prentice Hall, Englewood Cliffs, NJ.
- Farin, G., 1997. *Curves and Surfaces for Computer Aided Geometric Design*, 4th edition. Academic Press.
- Goldman, R., 2005. Curvature formulas for implicit curves and surfaces. *Computer Aided Geometric Design* 22 (7), 632–658.
- Hermann, T., 1996.  $G^2$  interpolation of free form curve networks by biquintic Gregory patches. *Computer Aided Geometric Design* 13, 873–893.
- Hogervorst, B.J., van Damme, R., 1993. Degenerate polynomial patches of degree 11 for almost  $G_2$  interpolation over triangles. *Numerical Algorithms* 5 (11), 557–568.
- Neamtu, M., Pfluger, P., 1994. Degenerate polynomial patches of degree 4 and 5 used for geometrically smooth interpolation in  $R_3$ . *Computer Aided Geometric Design* 11, 451–474.
- Pfluger, P.R., Neamtu, M., 1993. On degenerate surface patches. *Numerical Algorithms* 5 (11), 569–575.
- Reif, U., 1995. A note on degenerate triangular Bézier patches. *Computer Aided Geometric Design* 12, 547–550.
- Reif, U., 1998. TURBS—topologically unrestricted rational B-splines. *Constructive Approximation* 14, 57–77.
- Snyder, V., Hutchinson, J., 1902. *Differential and Integral Calculus*. American Book Company, New York. Chapter 14.
- Wolter, F.-E., Tuohy, S.T., 1991. Curvature computation for degenerate surface patches. *Computer Aided Geometric Design* 9, 241–270.
- Zheng, J., Sederberg, T.W., 2003. Gaussian and mean curvature of rational Bézier patches. *Computer Aided Geometric Design* 20, 297–301.